Endothelial nitric oxide synthase alterations are independent of turbulence in the aorta of patients with a unicuspid aortic valve

Brittany Balint, PhD, Catherine Kollmann, MD, Simon Gauer, MD, Jan M. Federspiel, MD, and Hans-Joachim Schäfers, MD, PhD

ABSTRACT

Objectives: Certain aortic valve malformations predispose to ascending aortic aneurysm, although the mechanisms are incompletely understood. The aim of this study was to determine whether turbulence across the unicuspid aortic valve (UAV) contributes to regional differences in endothelial nitric oxide (eNOS) signaling in the ascending aortic wall.

Methods: Samples were collected intraoperatively from the convex and concave ascending aortic wall from 64 patients with tricuspid aortic valves (TAVs; 25 nondilated, 17 dilated), or UAVs (9 nondilated, 13 dilated).

Results: In normal-sized aortas, eNOS protein was decreased in UAV compared with TAV ($P = .02$) whereas mRNA was similar ($P = .62$). eNOS protein was increased in UAV-dilated aortas compared with UAV-nondilated aortas ($P = .04$), whereas dilatation had no impact on eNOS protein levels in TAV aortas ($P = .73$). Comparing only aneurysmal aortas, we found no difference in eNOS mRNA or protein between dilated TAV and UAV aortas ($P = .26$, $P = .76$). For eNOS mRNA and protein levels in normal and dilated UAV-associated aortas, no differences were found between concavity and convexity (all $P > .05$). This differed from dilated TAV aortas, which showed decreased eNOS mRNA in the convexity ($P = .004$) whereas eNOS protein levels were similar ($P = .75$).

Conclusions: eNOS downregulation is observed in the UAV-associated ascending aorta and is apparently independent of dilatation. No regional differences were found, however, which would be expected if eNOS changes occur due to wall shear stress. This implies a congenital defect in eNOS signaling that may be stronger than turbulence-induced expression patterns. Further research should define the role of eNOS in aortopathy associated with aortic valve disease. (JTCVS Open 2021;8:157-69)

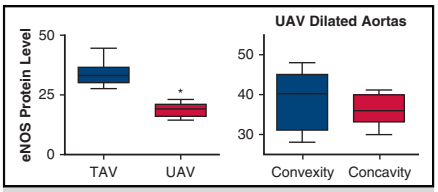

Regional assessment of UAV-associated aortas 13 suggests turbulence-independent eNOS changes.

CENTRAL MESSAGE

Altered eNOS in the aorta of unicuspid aortic valve patients is independent of turbulent flow, implying a genetic defect in eNOS signaling that is stronger than turbulence-induced expression patterns.

PERSPECTIVE

Altered eNOS is observed in the aortic wall of individuals with aortic valve disease, which may be related to genetic factors and/or turbulent flow. As altered eNOS occurs independent of turbulence in unicuspid aortic valve aortas, further studies are needed to determine the role of eNOS in aortopathy, and if it specifically contributes to the aggressive nature of unicuspid aortic valve aortopathy.

See Commentaries on pages 170, 172, 173, and 175.

Aortic valve (AV) malformations are associated with frequent occurrence of ascending aortic dilatation and dissection.[1] The probability of aortic aneurysm formation is up to 80-fold greater in individuals with a bicuspid aortic valve (BAV) compared with those with a normal (ie, tricuspid) aortic valve (TAV).[2] For individuals with a unicuspid aortic valve (UAV), a rarer variant, the risk of aortic complications may be even greater.[3]

The underlying mechanisms of AV-associated aortopathy are incompletely understood; both genetic and hemodynamic factors are possibly involved.[4-6] In a proportion of individuals with a BAV, well-recognized features of medial

From the Department of Thoracic and Cardiovascular Surgery, Saarland University Medical Center, Homburg/Saar, Germany.

This work was supported by institutional funding from Saarland University Medical Centre.

Received for publication Feb 24, 2021; accepted for publication Aug 16, 2021; available ahead of print Sept 4, 2021.

Address for reprints: Hans-Joachim Schäfers, MD, PhD, Department of Thoracic and Cardiovascular Surgery, Saarland University Medical Center, Kirrberger Str 100, 66424, Homburg/Saar, Germany (E-mail: h-j.schaefers@uks.eu).

2666-2736

https://doi.org/10.1016/j.xjon.2021.08.018

Abbreviations and Acronyms

AV = aortic valve
BAV = bicuspid aortic valve
eNOS = endothelial nitric oxide synthase
mRNA = messenger RNA
NOS3 = nitric oxide synthase 3
PCR = polymerase chain reaction
TAV = tricuspid aortic valve
UAV = unicuspid aortic valve

degeneration are observed in the aortic wall. Smooth muscle cell alterations are more severe in regions exposed to turbulence.[7] It remains a topic of debate, however, whether the turbulence related to the limited orifice area of the BAV causes dilatation or whether dilatation is a consequence of congenital aortic fragility.

Even less is known regarding UAV-associated aortopathy, in part because the UAV itself is rare and probably grossly underdiagnosed.[8] The UAV is a unicommissural valve with 2 hypoplastic commissures and 2 raphes.[9] It often presents as congenital aortic stenosis requiring treatment in infancy or childhood.[10] In adults with a UAV, surgical intervention for severe and prognostically relevant aortic stenosis is required at a younger age than those with BAVs or TAVs.[11] Prognostically relevant pathology associated with UAVs may also be primary valve incompetence. In addition, UAV-associated ascending aortic dilatation occurs at earlier ages compared with TAV and BAVs,[12-14] whereas its epidemiology is not yet well defined. So far, the mechanisms of UAV-associated aortic dilatation have not been well studied.

Similar to BAV, alterations of endothelial nitric oxide synthase (eNOS; NOS3) messenger RNA (mRNA) expression have been found in UAV aortas.[15] eNOS mRNA expression and protein levels can be regulated by wall shear stress,[16] and, thus, turbulence across the stenotic UAV may lead to altered eNOS expression in UAV aortas. It remains unknown, however, whether alterations in eNOS mRNA are accompanied by eNOS protein changes in UAV aortas. In addition, it is unclear whether changes in eNOS in the UAV aorta are flow-induced or genetically determined. If turbulence underlies eNOS alterations, regional variations of eNOS mRNA and/or protein should be expected.

In the current study, we compared levels of eNOS mRNA expression and protein levels in nondilated and dilated UAV aortas to that of TAV aortas. To assess for evidence of flow-induced dilatation, we additionally analyzed the mRNA expression and protein concentration of eNOS in regions susceptible to varying degrees of turbulence in the UAV-associated aortic wall.

METHODS

The data that support the findings of this study are available from the corresponding author upon reasonable request. This prospective study was conducted in accordance with the Declaration of Helsinki and was approved by the Ethics Committee in association with Saarland University Medical Center (Ethikkommission bei der Ärztekammer des Saarlandes, No. 205/10, Date of Issue: December 8, 2010). All patients gave written informed consent.

Samples

Ascending aortic tissue was extracted intraoperatively from 64 patients undergoing ascending aortic replacement or AV surgery. Patients with chronic viral diseases (eg, HIV, hepatitis B, hepatitis C) or with connective tissue disorders (eg, Marfan syndrome, Loeys–Dietz syndrome) were excluded. Aortic samples with macroscopic evidence of inflammatory disease (or atherosclerosis) were excluded. The samples were collected from both the outer wall (convexity) and the inner wall (concavity) of the ascending aorta 5 to 10 mm cranial to the sinotubular junction in all patients and also from the mid-ascending aorta in patients with a dilated aorta. AV morphology was determined preoperatively through transthoracic or transesophageal echocardiography and confirmed intraoperatively. The characteristic finding for UAV anatomy was hypoplasia of 2 commissures with concomitant cusp fusion adjacent to the hypoplastic commissures. Of the 64 patients enrolled in this study, 42 (65.6%) had a TAV and 22 (34.4%) had a UAV. Ascending aortic dimensions were determined by preoperative computed tomography and were measured a second time by intraoperative transesophageal echocardiography. If the ascending aortic diameter at either sampling site was larger than 40 mm,[17] the ascending aorta was considered dilated. Accordingly, aortic dilatation was present in 17 of 42 patients with a TAV and 13 of 22 patients with a UAV. Grouping of samples was based on AV morphology and maximal diameter of the ascending aorta: TAV nondilated (n = 25), TAV dilated (n = 17), UAV nondilated (n = 9), and UAV dilated (n = 13). Following extraction, whole aortic samples were divided and either immediately snap frozen in liquid nitrogen and stored at –80°C, or were placed in 4% phosphate-buffered formalin for fixation. Patient details and clinical characteristics are reported in Tables 1 and 2, respectively.

Real-Time Quantitative Reverse Transcription Polymerase Chain Reaction (PCR)

RNA isolation, reverse transcription, and quantitative real-time PCR were performed as previously described.[18] To summarize, RNA isolation was performed with the mirVana PARIS Kit (Ambion, Austin, Tex) and reverse transcription was achieved by using the High Capacity cDNA Reverse Transcription Kit (Applied Biosystems, Foster City, Calif) according to the manufacturers' instructions. Quantitative real-time PCR was performed on 96-well TaqMan Plates (Applied Biosystems), with TaqMan Gene Expression Assays (Applied Biosystems). All samples were run as triplicates. For patients with a UAV, the gene expression levels of NOS3 were analyzed relative to the mean expression level of NOS3 in aortic tissue from patients with a TAV and normal (nondilated) aortic dimensions (from the convex and concave walls) using eukaryotic transcription initiation factor 2B, subunit 1 (ie, EIF2B1), ETS-related transcription factor-1 (ie, ELF1), and hydroxymethylbilane synthase (ie, HMBS) as internal control genes. Previous studies have identified these gene targets as reference genes in aortic tissue samples from patients with various valve morphologies.[19] The expression level of NOS3 in nondilated TAV aortic tissue samples was set to 1. To assess for differences in expression levels between convex and concave regions of the aorta, relative expression of NOS3 normalized to the reference genes was compared within each patient. Mean differences in expression between the convexity and concavity were determined for each patient cohort and then compared within groups. Relative quantification values for NOS3 expression were determined with the 2^{-DDCT} method.

TABLE 1. Patient characteristics based on aortic valve morphology

	Tricuspid	Unicuspid	*P* value
Number	42	22	
Age, y ± range	62.4 ± 13.5	37.8 ± 13.0	<.0001*
Sex, % male	69.4	76.2	.76
Aortic valve pathology, n (%)			
Stenosis	10 (23.8)	4 (18.2)	.61
Insufficiency	28 (66.7)	9 (40.9)	.05
Combined	4 (9.5)	8 (36.3)	.009*
Comorbidities, n (%)			
Hypertension	21 (50.0)	3 (13.6)	.004*
Diabetes mellitus	3 (7.1)	0 (0)	.14
Hyperlipidemia	5 (11.5)	0 (0)	.09
Coronary artery disease	12 (28.6)	1 (4.5)	.02*
Medication, n (%)			
β-blocker	20 (47.6)	6 (27.3)	.12
Angiotensin-converting enzyme inhibitor	16 (38.0)	5 (22.7)	.22
Angiotensin 1-receptor agonist	9 (16.3)	1 (4.5)	.08
Diuretic	11 (26.2)	1 (4.5)	.04*
Insulin	3 (7.1)	0 (0)	.20
Calcium channel blocker	10 (23.8)	1 (4.5)	.06
Statin	12 (28.6)	0 (0)	.001*
Aldosterone antagonist	7 (16.7)	1 (4.5)	.16

*$P < .05$.

Protein Quantification

Quantification of eNOS protein levels in ascending aortic tissue was carried out as previously described.[18] To summarize, protein isolation was achieved through the Protein Quant Sample Lysis Kit (Life Technologies, Carlsbad, Calif). Protein expression of eNOS was determined by Western Blot analysis, using polyacrylamide Bis-Tris 4%-12% gels (Life Technologies). Primary antibodies were used to assess for eNOS (Anti-eNOS/NOS Type III Mouse, 1:1.000; BD Transduction Laboratories, Franklin Lakes, NJ) and β-actin (β-actin 8H10D10 mouse monoclonal antibody, 1:200.000; Cell Signaling Technology, Danvers, Mass). Antibodies were visualized with peroxidase-conjugated AffiniPure Goat Anti-Mouse immunoglobulin G (1:1.000; Jackson ImmunoResearch, West Grove, Pa) and were detected by chemiluminescent staining (Pierce ECL Western Blotting Substrate; Thermo Scientific, Waltham, Mass). eNOS levels were normalized to β-actin concentration within each patient sample triplicate. To assess for differences in eNOS levels between convex and concave regions of the aorta, relative eNOS concentration (eNOS/β-actin) was compared between the convexity and the concavity within each patient sample, and further compared within patient groups.

TABLE 2. Patient characteristics based on aortic diameter

	Tricuspid		Unicuspid	
	Normal	Dilated	Normal	Dilated
Number	25	17	9	13
Age, y ± range	67.8 ± 7.0	56.3 ± 6.1	31.9 ± 5.8	43.4 ± 5.6
Sex; % male	26.6	84.2	66.6	84.6
Maximal ascending aortic diameter				
Mean ± standard deviation	3.1 ± 4.5	5.4 ± 4.9	3.1 ± 1.8	4.9 ± 4.3
Range	2.3-3.9	4.1-8.0	2.0-3.9	4.2-5.7

Immunohistochemistry

Formalin-fixed, paraffin-embedded aortic tissue was section into 1-μm slices and then immunolabeled with either total eNOS (1:30; Cell Signaling Technology) or phosphorylated eNOS (1:50; Abcam). Primary antibodies were visualized with fluorescent conjugated secondary antibodies (goat anti-mouse-594, or goat anti-rabbit-647). Tissue sections were counterstained with DAPI. Images were taken with a laser scanning confocal microscope (Zeiss LSM, Plan Apochromat 40 × 1.3 oil objective). For both stains, 10 regions of interest were captured from each patient. Total eNOS and phosphorylated eNOS were measured by fluorescence intensity with ImageJ (National Institutes of Health, Bethesda, Md).

Statistical Analysis

All statistical analyses were carried out using Prism 7 (GraphPad Software, San Diego, Calif). All data sets were tested for normality by the D'Agostino and Pearson omnibus test. In the case of normal distributions, comparisons were made with the Student *t* test. Nonparametric distributions were compared by the Mann–Whitney *U* test. Categorical variables were compared using χ^2 tests. Data are presented as mean ± standard deviation.

RESULTS

Total eNOS and Phosphorylated eNOS Protein Changes in UAV Versus TAV Aortas

Ascending aortic tissue was obtained from a total of 64 patients. Clinical characteristics for each patient group are presented in Tables 1 and 2.

To understand the role of eNOS in the normal UAV aortic wall, we first analyzed eNOS levels in nondilated aortic tissue. There was no difference in eNOS mRNA expression between the UAV and TAV nondilated aortas (1.3 ± 1.8 vs 1.3 ± 1.0, $P = .62$; Figure 1, *A*). Despite having normal-sized aortas, however, eNOS protein concentration was decreased in UAV aortas compared with TAVs (19.3 ± 9.9 vs 36.6 ± 36.0, $P = .02$; Figure 1, *B*). Immunohistochemistry revealed that eNOS protein was decreased in the intima and the media of UAV nondilated aortas ($P = .04$ and .03, respectively), but no differences were observed in adventitial eNOS ($P = .81$; Figure 1, *C*). Interestingly, however, phosphorylated eNOS/total eNOS (p-/total eNOS) expression was increased in the aortic media of patients with a UAV compared with a TAV ($P < .0001$; Figure 1, *D*). No difference was observed in p-/total eNOS in the intima or the adventitia of nondilated UAV aortas ($P = .42$, .32, respectively; Figure 1, *D*).

To determine whether dilatation itself impacts eNOS, we then compared normal and aneurysmal aortas within each AV group. For individuals with a TAV, eNOS mRNA expression (1.0 ± 2.0 vs 1.2 ± 0.6, $P = .69$) and protein concentration (30.8 ± 22.0 vs 33.2 ± 15.9; $P = .72$) did not differ between normal-sized and aneurysmal aortas (Figure 2, *A* and *B*). Likewise, no differences were observed in eNOS protein levels in the intima, media, or adventitia between normal and dilated TAV aortas ($P = .12$, .33, .71, respectively; Figure 2, *C*). Interestingly, there was a significant increase in p-/total eNOS concentration in the intimal

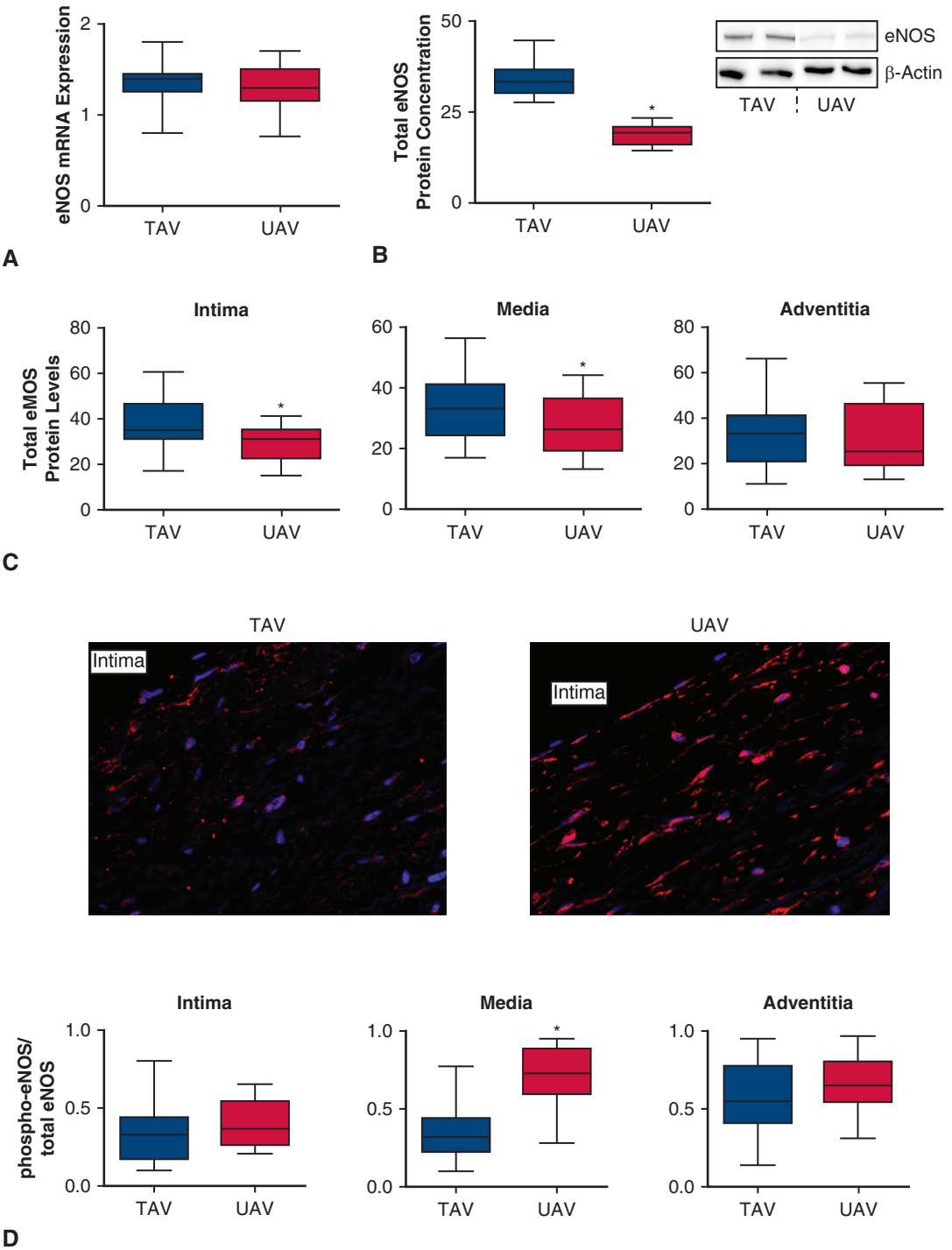

FIGURE 1. Endothelial nitric oxide synthase (*eNOS*) protein levels are downregulated in the UAV-associated nondilated ascending aorta, whereas phosphorylated eNOS is increased in the media layer. A, *Box and whisker plot* depicting the mRNA expression of NOS3 (eNOS) in TAV- and UAV-associated ascending aortic tissue from normal (nondilated) ascending aortas ($P = .62$). B, *Box and whisker plot* and representative *Western blot* images depicting the decreased protein concentration of eNOS in UAV-associated ascending aortic tissue compared with TAV from normal (nondilated) ascending aortas ($P = .02$). C, *Box and whisker plots* depicting total eNOS protein levels in the intima ($P = .04$), media ($P = .03$), and adventitia ($P = .81$) from nondilated TAV and UAV aortas. D, *Top*: Fluorescent images of ascending aortic tissue stained for phosphorylated-eNOS (*red*) and counterstained with DAPI to detect the nuclei (*blue*). The intimal layer is labeled (*top left corner*). *Bottom*: *Box and whisker plots* depicting the ratio of phosphorylated-eNOS/total eNOS levels in the intima ($P = .42$), media ($P < .0001$), and adventitia ($P = .32$) from nondilated TAV and UAV aortas. *Box and whisker plots* display the median (*middle bar*), the maximum and minimum values (*upper and lower bars*, respectively), and the first and third quartile (*bottom lines* and *top lines of box*, respectively).

layer of dilated TAV aortas compared to nondilated ($P = .0007$), but not in the media or adventitia ($P = .82$, .12, respectively; Figure 2, *D*).

In UAV aortas, however, eNOS mRNA expression was similar between nondilated and dilated UAV aortas (1.3 ± 0.6 vs 1.3 ± 0.4, $P = .80$), but eNOS protein levels were increased with dilatation (17.8 ± 7.5 vs 36.9 ± 23.8, $P = .04$; Figure 3, *A* and *B*). Immunohistochemistry revealed that eNOS was increased in the intima and the media ($P = .002$, .004, respectively), but not in the adventitial layer ($P = .32$, Figure 3, *C*). The p-/total eNOS levels were increased in all 3 layers of the dilated UAV aorta (intima: $P = .0006$, media: $P = .03$, adventitia: $P = .02$; Figure 3, *D*). Accordingly, when we compared aneurysmal aortic tissue from TAV and UAV individuals, eNOS mRNA expression was similar between dilated UAV and TAV aortas (1.7 ± 0.72 vs 1.4 ± 0.4, $P = .26$). Likewise, in contrast to the nondilated aortas, there was no difference in eNOS protein level between UAV and TAV (35.1 ± 16.8 vs 32.3 ± 26, $P = .76$). In UAV dilated aortas, however, there was a significant increase in p-/total eNOS in the media layer compared to that of dilated TAV aortas ($P = .011$). Thus, eNOS protein downregulation in UAV aortas is observed in the absence of dilatation, whereas in dilated aortas no difference in total eNOS was observed between the different AV morphologies.

Patients with a UAV tend to require surgical intervention before those with a TAV. Therefore, the patients with a UAV were significantly younger than the patients with a TAV in this study ($P < .0001$; Figure E1, *A*). To correct for age, we performed a subanalysis in which the 10 oldest patients with TAV and the 5 youngest patients with UAV were removed from the dataset, which yielded a patient population with similar ages between groups ($P = .08$; Figure E1, *B*). Comparing total eNOS mRNA and protein levels between groups in the subanalysis yielded similar results to the entire data set (Figure E1, *C* and *D*). Mainly, eNOS protein concentration was decreased in normal UAV aortas versus normal TAV aortas ($P = .003$), and eNOS protein levels were increased in dilated versus normal UAV aortas ($P = .011$; Figure E1, *D*). No significant differences were observed between groups in the subanalysis ($P > .05$; Figure E1, *D*).

Regional Differences in eNOS Expression in TAV, but not UAV, Dilated Aortas

To determine whether turbulence impacts eNOS signaling in the ascending aorta, we measured eNOS mRNA expression and protein levels in regions susceptible to wall shear stress changes in normal and dilated aortas. In nondilated aortas from individuals with a TAV, eNOS mRNA expression was similar in the convex and concave walls of the ascending aorta (2.1 ± 2.5 vs 1.9 ± 1.5; $P = .73$; Figure 4, *A*). Similarly, no regional differences in eNOS protein levels were detected in nondilated TAV aortas (convexity: 32.8 ± 26.5, concavity: 35.5 ± 21.0; $P = .71$; Figure 4, *A*). Accordingly, total eNOS and p-/total eNOS levels were unchanged between the convex and concave walls in all 3 layers of the nondilated TAV aorta (intima: $P = .23$, .13, media: $P = .06$, .15, adventitia: $P = .22$, .17). Interestingly, however, eNOS mRNA expression in dilated TAV aortas was decreased in the convexity compared to the concavity of the aortic wall adjacent to the sinotubular junction (2.2 ± 1.2 vs 3.6 ± 1.2; $P = .004$; Figure 4, *B*) and in the mid-ascending aorta (2.0 ± 1.2 vs 3.8 ± 2.0; $P = .004$; Figure 4, *C*). Regional differences in protein expression, however, were not detected in TAV dilated aortas at either the level of the sinotubular junction (29.9 ± 13.6 vs 32.3 ± 27.6; $P = .75$; Figure 4, *B*), or in the mid-ascending aorta (33.1 ± 33.2 vs 28.5 ± 27.6; $P = .67$; Figure 4, *C*). Likewise, total eNOS and p-/total eNOS levels were unchanged between the convex and concave walls in the intima, media, and adventitia of the dilated TAV aorta (intima: $P = .16$, .23, media: $P = .11$, .46, adventitia: $P = .71$, .37).

As the UAV is related to a high degree of turbulence, we expected more pronounced regional differences in eNOS in the UAV-associated aortic wall. In nondilated UAV aortas, however, eNOS mRNA expression (2.2 ± 1.2 vs 2.0 ± 1.2; $P = .89$) and protein concentration (33.0 ± 9.3 vs 29.5 ± 20.7; $P = .87$) were similar between the convex and concave walls of the ascending aorta (Figure 5, *A*). Accordingly, total eNOS and p-/total eNOS levels were unchanged between the convex and concave walls in all 3 layers of the nondilated UAV aorta (intima: $P = .65$, .21, media: $P = .17$, .81, adventitia: $P = .11$, .21). Similar results were found in dilated UAV aortas. At the level of the sinotubular junction, there were no differences in eNOS mRNA expression (2.9 ± 1.4 vs 2.8 ± 1.8; $P = .12$) or protein concentration (41.9 ± 38.8 vs 32.9 ± 29.2; $P = .33$) in the convexity and the concavity of the dilated aortic wall (Figure 5, *B*). Likewise, there was no difference in eNOS mRNA expression (4.1 ± 0.7 vs 3.6 ± 5.4; $P = .10$) or protein concentration (33.7 ± 28.9 vs 29.7 ± 19.4; $P = .14$) between the convexity and the concavity of the dilated mid-ascending aortic wall from UAV patients (Figure 5, *C*). Likewise, total eNOS and p-/total eNOS

eNOS mRNA expression values are normalized to the mean value of 3 internal control genes (EIF2B1, ELF1, and HMBS), and then to the mean expression value in TAV nondilated aortas. eNOS protein expression values are normalized to beta-actin protein expression. Statistical comparisons were performed with the Student *t* test (for normal distributions) and the Mann–Whitney *U* test (for nonparametric distributions). *$P < .05$; TAV: n = 25, UAV: n = 9. *mRNA*, Messenger RNA; *TAV*, tricuspid aortic valve; *UAV*, unicuspid aortic valve.

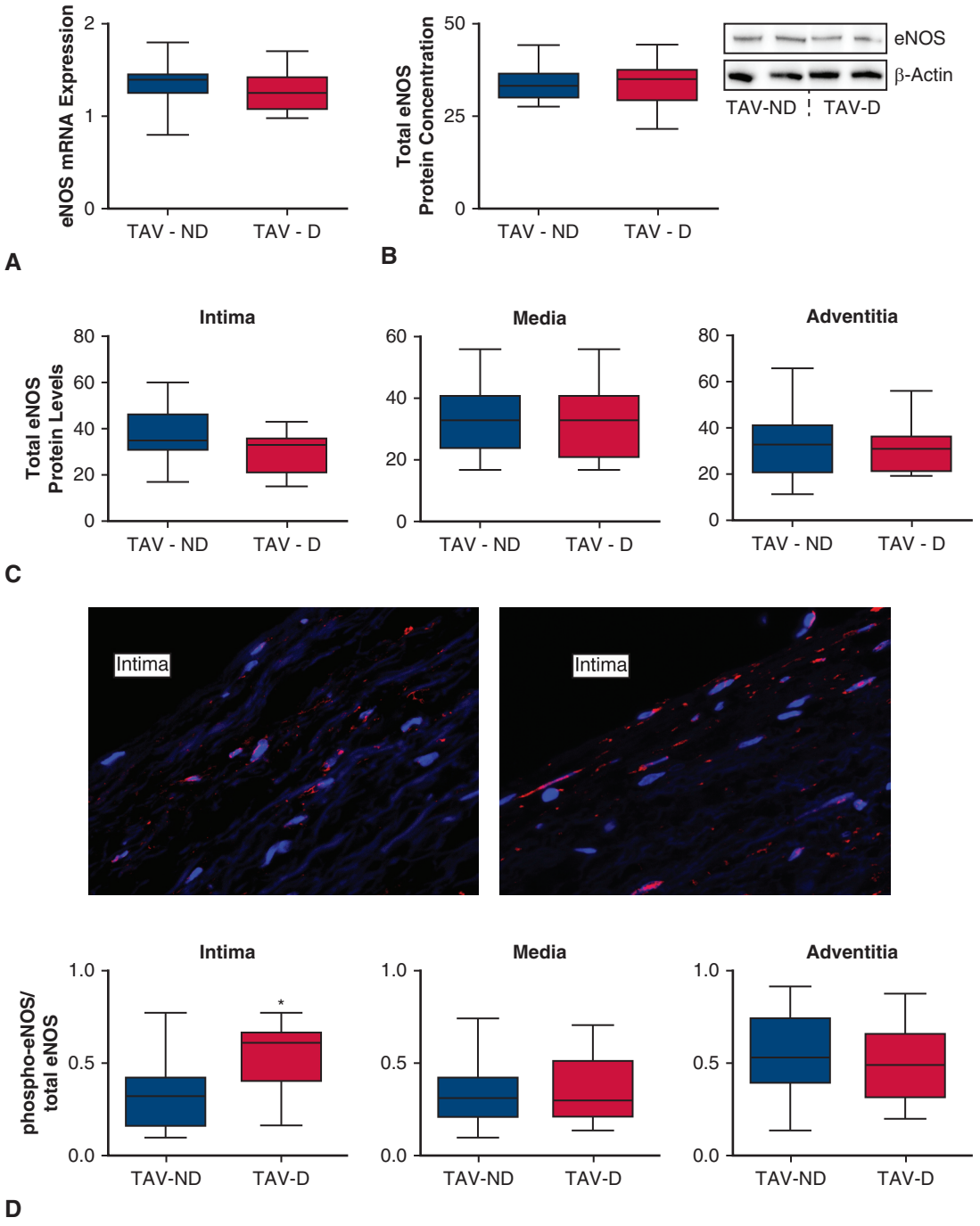

FIGURE 2. Phosphorylated endothelial nitric oxide synthase (*eNOS*) protein levels are increased in the intima of dilated versus normal aortas from patients with normal (ie, tricuspid) aortic valves. A, *Box and whisker plot* depicting the mRNA expression of NOS3 (eNOS) in normal (*ND*; nondilated) and dilated (*D*) ascending aortas from individuals with a tricuspid aortic valve (*TAV*) ; $P = .69$). B, *Box and whisker plot* and representative *Western blot* images depicting the protein concentration of eNOS in TAV-ND and TAV-D ascending aortas ($P = .72$). C, *Box and whisker plots* depicting total eNOS protein levels in the intima ($P = .12$), media ($P = .33$), and adventitia ($P = .71$) from normal (ND; nondilated) and dilated (D) TAV aortas. D, *Top*: Fluorescent images of ascending aortic tissue stained for phosphorylated-eNOS (*red*) and counterstained with DAPI to detect the nuclei (*blue*). The intimal layer is labeled (*top left corner*). *Bottom*: *Box and whisker plots* depicting the ratio of phosphorylated-eNOS/total eNOS levels in the intima ($P = .0007$), media ($P = .82$), and adventitia ($P = .12$) from normal and dilated TAV aortas. *Box and whisker plots* display the median (*middle bar*), the maximum and minimum values (*upper* and *lower bars*, respectively), and the first and third quartile (*bottom lines* and *top lines of box*, respectively). eNOS mRNA expression values are normalized to the mean value of 3 internal control genes (EIF2B1, ELF1, and HMBS), and then to the mean expression value in TAV nondilated aortas. eNOS protein expression values are normalized to beta-actin protein expression. Statistical comparisons were performed with the Student *t* test (for normal distributions) and the Mann–Whitney *U* test (for nonparametric distributions). *$P < .05$; TAV-ND: n = 25, TAV-D: n = 17. *mRNA*, Messenger RNA.

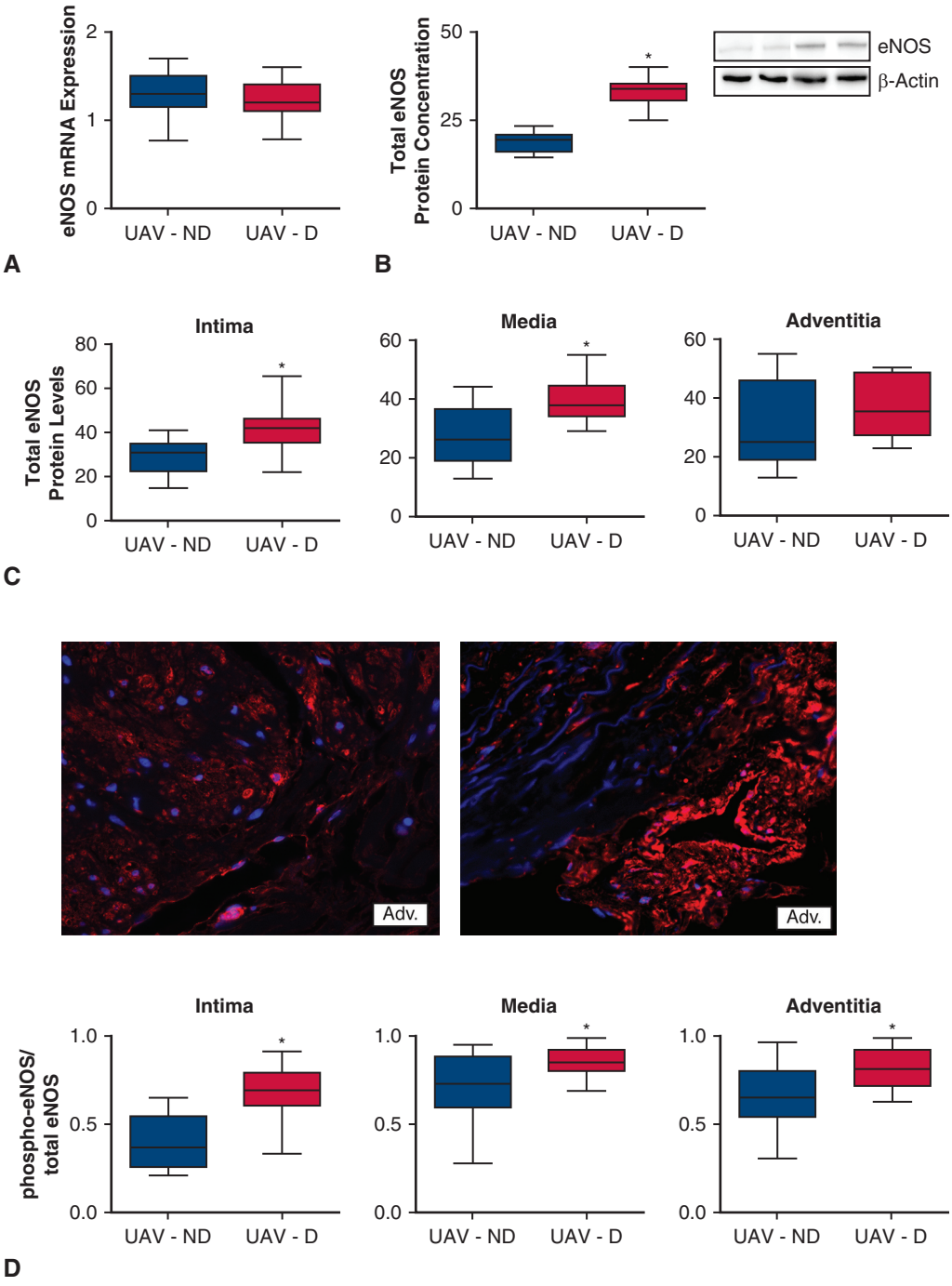

FIGURE 3. Total and phosphorylated eNOS are increased with dilatation in the ascending aorta of individuals with a unicuspid aortic valve. A, *Box and whisker plot* depicting the mRNA expression of NOS3 (eNOS) in normal (*ND*; nondilated) and dilated (*D*) ascending aortas from individuals with a unicuspid aortic valve (UAV; $P = .80$). B, *Box and whisker plot* and representative *Western blot* images depicting the protein concentration of eNOS in UAV-ND and TAV-D ascending aortas ($P = .04$). C, *Box and whisker plots* depicting total eNOS protein levels in the intima ($P = .002$), media ($P = .004$), and adventitia ($P = .32$) from normal and dilated UAV aortas. D, *Top*: Fluorescent images of ascending aortic tissue stained for phosphorylated-eNOS (*red*) and counterstained with DAPI to detect the nuclei (*blue*). The intimal layer is labeled (*top left corner*). *Bottom*: *Box and whisker plots* depicting the ratio of phosphorylated-eNOS/total eNOS levels in the intima ($P = .0006$), media ($P = .03$), and adventitia ($P = .02$) from normal and dilated UAV aortas. *Box and whisker plots* display the median (*middle bar*), the maximum and minimum values (*upper and lower bars*, respectively), and the first and third quartile (*bottom lines and top lines of box*, respectively). eNOS mRNA expression values are normalized to the mean value of 3 internal control genes (EIF2B1, ELF1, and HMBS), and then to the mean expression value in TAV nondilated aortas. eNOS protein expression values are normalized to beta-actin protein expression. Statistical comparisons were performed by the Student *t* test (for normal distributions) and the Mann–Whitney *U* test (for nonparametric distributions). *$P < .05$; UAV: normal: n = 9, dilated: n = 13. *eNOS*, Endothelial nitric oxide synthase; *mRNA*, messenger RNA; *UAV*, unicuspid aortic valve.

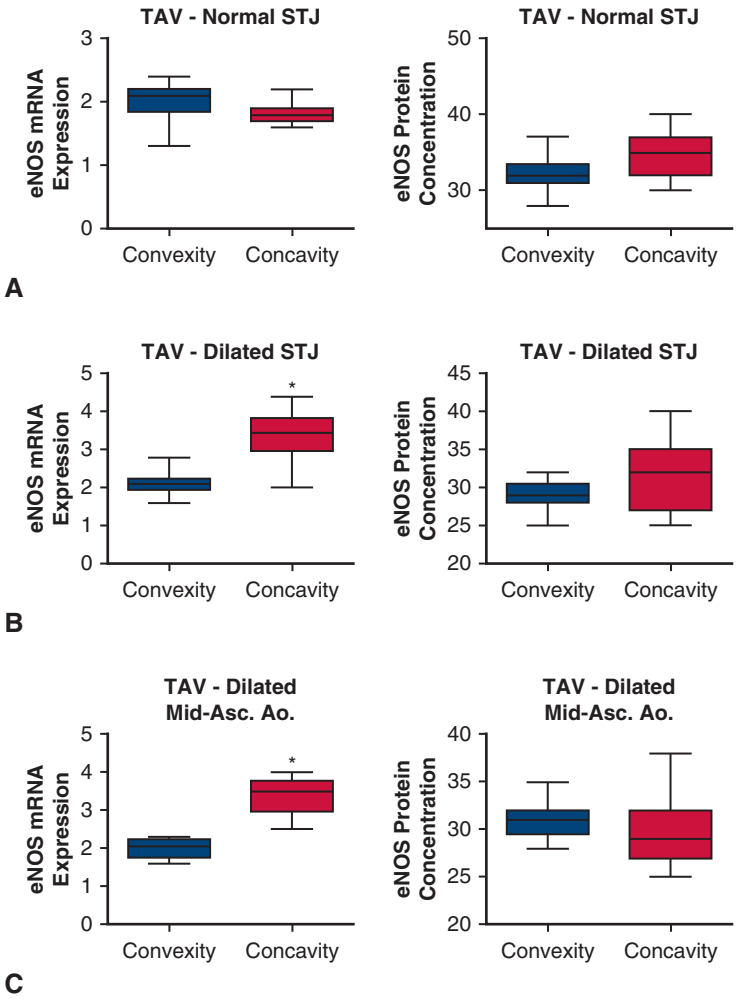

FIGURE 4. Endothelial nitric oxide synthase (*eNOS*) expression is decreased in the convexity of the aortic wall in tricuspid aortic valve (*TAV*)-associated aortas. A, *Box and whisker plots* depicting the mRNA expression of NOS3 (eNOS; *left*; $P = .73$) and the protein concentration of eNOS (*right*; $P = .71$) in the convexity and the concavity of TAV-associated nondilated aortas at the level of the sinotubular junction (*STJ*). B-C, *Box and whisker plots* depicting the mRNA expression (*left*; $P = .004$) and the protein concentration of eNOS (*right*; $P = .75$) in the convexity and the concavity of TAV associated dilated aortas (B) at the level of the STJ, and (C) at the level of the mid-ascending aorta (*Mid-Asc. Ao.*); mRNA: *left*; $P = .004$, protein: *right*; $P = .67$). *Box and whisker plots* display the median (*middle bar*), the maximum and minimum values (*upper and lower bars*, respectively), and the first and third quartile (*bottom lines and top lines of box*, respectively). eNOS mRNA expression values are normalized to the mean value of 3 internal control genes (EIF2B1, ELF1, and HMBS). eNOS protein expression values are normalized to beta-actin protein expression. Statistical comparisons were performed with the Student *t* test (for normal distributions) and the Mann–Whitney *U* test (for nonparametric distributions). TAV: nondilated: n = 25, dilated: n = 17. $*P < .05$. *mRNA*, Messenger RNA.

levels were unchanged between the convex and concave walls in all 3 layers of the dilated UAV aorta, at the level of the STJ (intima: $P = .55, .89$, media: $P = .31, .44$, adventitia: $P = .77, .71$) and the mid-ascending aorta (intima: $P = .33, .23$, media: $P = .11, .91$, adventitia: $P = .69, .41$). These findings suggest that turbulence itself does not alter eNOS expression or activation in the UAV-associated ascending aortic wall.

DISCUSSION

AV malformation, ie bicuspid valve morphology, is associated with aortic dilatation, yet the underlying mechanisms remain uncertain. Although turbulent flow and subsequent shear stress changes in the aortic wall may play a role, some evidence suggests that genetic factors are involved.[20] As flow across the UAV tends to be even more turbulent, however, we assumed that turbulence could play an even more important role in UAV aortopathy compared with aneurysms associated with normal (ie, TAV) AVs. As eNOS signaling is regulated by wall shear stress, we assessed for eNOS mRNA expression and protein levels in regions where variations in wall shear stress are suspected.

Altered eNOS signaling has been observed in BAV-associated ascending aortas.[15,18,21-23] Although its role is

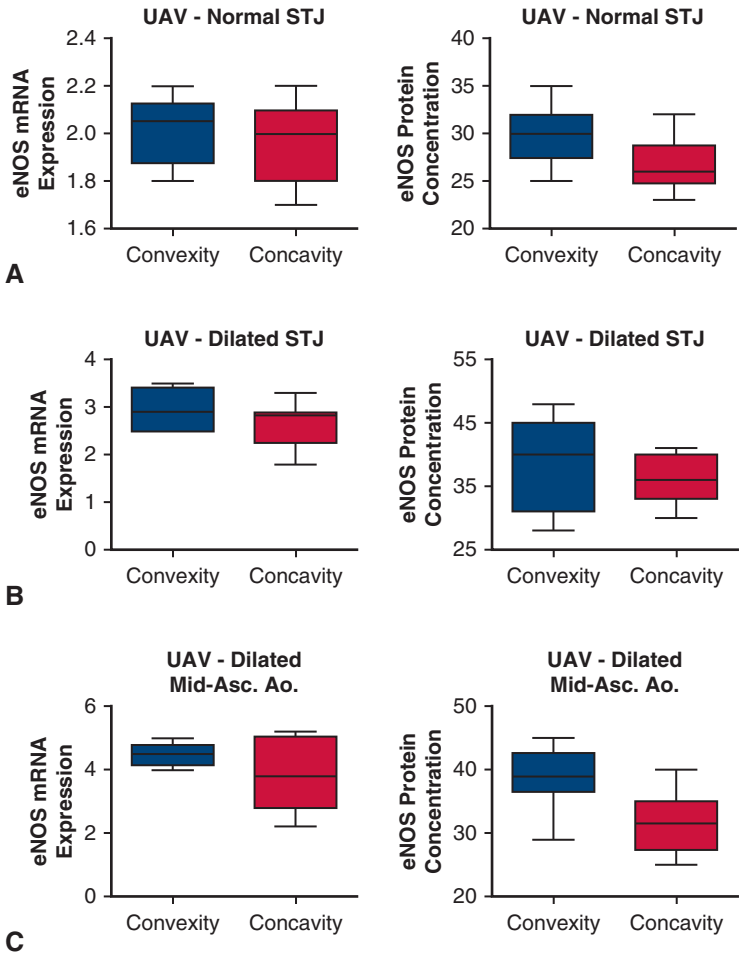

FIGURE 5. Endothelial nitric oxide synthase (*eNOS*) is similar in the convex and concave aortic walls in unicuspid aortic valve (*UAV*)-associated aortas. A, *Box and whisker plots* depicting the mRNA expression of NOS3 (eNOS; *left*; $P = .12$) and the protein concentration of eNOS (*right*; $P = .13$) in the convexity and the concavity of unicuspid aortic valve (UAV)-associated nondilated aortas at the level of the sinotubular junction (*STJ*). B-C, *Box and whisker plots* depicting the mRNA expression (*left*; $P = .89$) and the protein concentration of eNOS (*right*; $P = .87$) in the convexity and the concavity of UAV associated dilated aortas (B) at the level of the sinotubular junction, and (C) at the level of the mid-ascending aorta (*Mid-Asc. Ao.*); mRNA: *left*; $P = .10$, protein: *right*; $P = .14$). *Box and whisker plots* display the median (*middle bar*), the maximum and minimum values (*upper and lower bars*, respectively), and the first and third quartile (*bottom lines and top lines of box*, respectively). eNOS mRNA expression values are normalized to the mean value of 3 internal control genes (EIF2B1, ELF1, and HMBS). eNOS protein expression values are normalized to beta-actin protein expression. Statistical comparisons were performed by the Student *t* test (for normal distributions) and the Mann–Whitney *U* test (for nonparametric distributions). Data are presented as mean (bars) ± standard error of the mean (error bars). UAV: nondilated: n = 9, dilated: n = 13. $*P < .05$. *mRNA*, Messenger RNA.

unclear, eNOS may be involved in extracellular matrix remodeling within the aortic wall. In buckled arteries, for instance, eNOS protein levels were decreased alongside increased matrix metalloproteinase 2 levels and a reduction in collagen content.[24] Furthermore, eNOS knockout mice had reduced elastin protein expression and increased matrix metalloproteinase-2 and -9 activity.[25] It is uncertain, however, whether eNOS plays a direct role in aortic dilatation associated with UAVs.

Most BAV studies have analyzed either mRNA expression[15,21] or protein concentration[22,23] of eNOS. Results have been inconsistent. Furthermore, it remains unclear whether eNOS dysregulation occurs in response to dilatation, as previous studies do not always distinguish between normal and dilated aortas.[21-23] Alterations in eNOS mRNA expression were also found in UAV-associated aortas,[15] but protein levels have yet to be studied. In light of these inconsistencies, we assessed for both mRNA expression and protein levels of eNOS and activated eNOS (p-eNOS; phosphorylated eNOS) in normal-sized and dilated UAV aortas. To determine whether turbulence alters eNOS in UAV aortas, we also analyzed eNOS mRNA and protein in different regions of the aortic wall where variations in wall shear stress are suspected.

In our current study, eNOS protein levels in the intima and media layers were decreased in the UAV nondilated

aorta compared with that of TAV. This is similar to findings in BAV aortas.[18,23] Furthermore, p-eNOS was increased in the medial layer of nondilated UAV aortas. These findings suggest that dysregulated eNOS signaling in the UAV aorta occurs in the absence of aortic dilatation. It is possible that congenital changes in eNOS signaling in the aortic wall contribute to aortic wall remodeling and provoke later aortic dilatation in UAV aortas. Interestingly, when studying aneurysmal aortic tissue from individuals with a UAV, we found no difference in either eNOS mRNA expression or protein levels compared with that of TAVs. This is similar to previous work that showed similar eNOS mRNA expression between UAV, BAV, and TAV aortas when only aneurysmal tissue was included.[15] These findings suggest that eNOS could be part of advanced changes in the nondilated ascending aortic wall that contribute to later aneurysm formation in individuals with a UAV.

It is important to note that the difference in eNOS protein levels between UAV and TAV aortas disappears in the case of aneurysmal tissue because eNOS protein levels were increased in association with dilatation in the UAV ascending aorta. This response to dilatation was also observed in BAV aortas[18] but not in TAV aortas. This could indicate that AV malformations are associated with unstable eNOS signaling in the ascending aorta that is further altered by aortic remodeling to the point of obvious aneurysm. Additional studies are required to determine the role of eNOS in aortic remodeling and subsequent dilatation in UAV-associated aortas.

Studies have clearly revealed alterations in blood flow patterns and subsequent shifts in wall shear stress in BAV aortas.[26,27] Yet, alterations in eNOS were not observed in regions susceptible to turbulence in the BAV aorta.[18] In general, blood flow across the UAV is exceedingly more turbulent compared to the BAV,[28] likely due in part to its stenotic nature.[29] Furthermore, severe valve dysfunction occurs earlier and progresses faster in individuals with a UAV compared with individuals with a BAV,[10] including aortic dilatation.[30] In the current study, the majority of TAV patients presented with aortic insufficiency, whereas the majority of patients with UAV had both aortic insufficiency and aortic stenosis. The added component of aortic stenosis in UAV aortas likely further impacts wall shear stress.[29] Therefore, we tested the hypothesis that remarkably turbulent flow associated with the UAV is responsible for alterations in eNOS signaling in the UAV-associated ascending aortic wall, which may provoke accelerated aging in the aorta. Like in the BAV aorta,[18] however, we did not detect any regional differences in either mRNA expression or protein levels of eNOS in the UAV-associated aortic wall. These results, paired with our findings of altered eNOS in nondilated aortas, imply that dysregulated eNOS signaling in the UAV aorta occurs independent of turbulence. These findings suggest an underlying genetic defect in eNOS signaling in the UAV-associated aorta that may be similar to that of BAV aortas. Genetic changes in eNOS have already been shown to contribute to BAV formation in mice.[31] Further studies should be employed to evaluate whether genetic changes in eNOS can be detected in the formation of the UAV or in the UAV ascending aorta.

In contrast, regional differences in eNOS mRNA expression were observed in the dilated TAV aorta. Although data regarding turbulence associated with the TAV are limited, it has been suggested that elongation of the aorta occurs concurrently in a portion of cases of aortic dilatation, and is associated with a heightened risk of adverse aortic events.[32] Elongation of the aorta may result in angular changes between the left ventricular outflow tract and the aortic root[33] and may produce abnormal flow patterns extending to the ascending aorta. Interestingly, p-eNOS was increased in the aortic intima of dilated TAV aortas, which may suggest flow-mediated changes to the intimal layer associated with dilatation in TAV aortas. Further work is required to determine whether elongation of the TAV-associated aorta produces turbulence, and whether this could be responsible for the differences in eNOS mRNA expression in dilated TAV aortas.

In summary, we have shown that dysregulated eNOS signaling exists in the UAV-associated aorta. Interestingly, however, alterations in total eNOS mRNA expression and protein levels, as well as phosphorylated eNOS, occur before dilatation in UAV aortas, and independent of alterations in aortic wall shear stress (Figure 6). These findings imply that eNOS signaling is regulated independent of turbulence in the UAV aortic wall and is likely caused by a congenital defect in eNOS signaling that is stronger than turbulence-induced expression patterns. Moreover, since aortopathy associated with the UAV is more aggressive than that of the TAV or BAV, further studies are required to determine the role of eNOS in UAV aortopathy and whether additional factors contribute to accelerated aging in the UAV aortic wall.

Limitations

As the UAV is a rare variant of AV malformations, it was difficult to achieve a larger population size for this study. Furthermore, patients with a UAV tend to require surgical intervention for aortic complications earlier in life. This resulted in a limited sample size with a younger mean age, differences in valve lesion pathology, and some comorbidities and medications. Despite these obstacles, however, we were able to obtain a meaningful population size for both UAV normal and dilated aortas that allowed for the detection of altered eNOS signaling compared with TAV aortas with statistical significance. Furthermore, our subanalysis, which evaluated age-matched populations from TAV and UAV individuals, revealed similar findings compared with analyses that included the entire study population. Therefore, despite

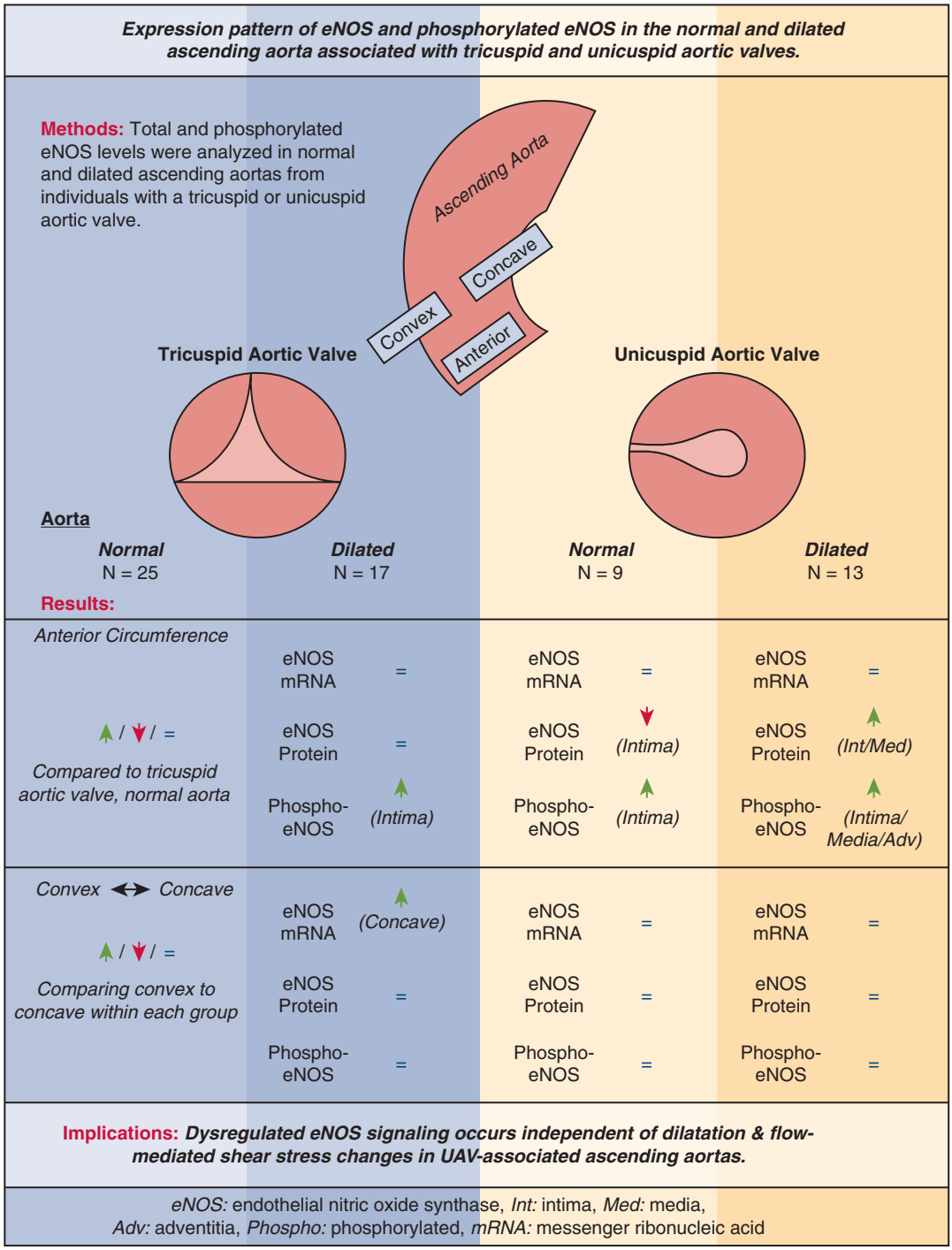

FIGURE 6. The expression patterns of endothelial nitric oxide synthase (*eNOS*) and phosphorylated eNOS in the normal and dilated ascending aorta associated with tricuspid and unicuspid aortic valves. Tissue samples were taken from the convex, concave and anterior walls of normal or dilated ascending aortas from individuals with a tricuspid aortic valve (TAV) or with a unicuspid aortic valve (UAV). At the anterior circumference, the total eNOS (endothelial nitric oxide synthase) mRNA and protein were measured and compared between groups. eNOS mRNA was unchanged (=) between groups, whereas eNOS protein was decreased (↓) in the intimal layer of normal-sized UAV aortas. eNOS protein increased (↑) in the intimal and medial layers with dilatation in the UAV aortas. Phosphorylated-eNOS (p-eNOS) was also measured at the anterior circumference. In dilated TAV aortas, p-eNOS was increased in the intima (*Int*). In UAV aortas, p-eNOS was increased in the medial layer, and it was increased in the intima, media (*Med*) and adventitia (*Adv*) of dilated UAV aortas. Total eNOS mRNA and protein and p-eNOS protein were compared at the convexity and the concavity within each aorta. In dilated TAV aortas, eNOS mRNA was increased at the concavity versus the convexity. No other changes were observed when comparing the convex and concave walls of the aorta for either group. =: no statistical difference between groups ($P \geq .05$). ↑: increased value with statistical significance ($P < .05$). ↓: decreased value with statistical significance ($P < .05$). *mRNA*, Messenger RNA.

being younger, this exploratory pilot study provides evidence to suggest turbulence-independent changes in eNOS signaling in UAV aortas.

Conflict of Interest Statement

The authors reported no conflicts of interest.

The *Journal* policy requires editors and reviewers to disclose conflicts of interest and to decline handling or reviewing manuscripts for which they may have a conflict of interest. The editors and reviewers of this article have no conflicts of interest.

References

1. Erbel R, Aboyans V, Boileau C, Bossone E, Bartolomeo RD, Eggebrecht H, et al; Guidelines ESC Committee for Practice Guidelines. 2014 ESC Guidelines on the diagnosis and treatment of aortic diseases: document covering acute and chronic aortic diseases of the thoracic and abdominal aorta of the adult. The task force for the diagnosis and treatment of aortic diseases of the European Society of Cardiology (ESC). *Eur Heart J*. 2014;35:2873-926.
2. Michelena HI, Prakash SK, Della Corte A, Bissell MM, Anavekar N, Mathieu P, et al. Bicuspid aortic valve: identifying knowledge gaps and rising to the challenge from the International Bicuspid Aortic Valve Consortium (BAVCon). *Circulation*. 2014;129:2691-704.
3. Larson EW, Edwards WD. Risk factors for aortic dissection: a necropsy study of 161 cases. *Am J Cardiol*. 1984;53:849-55.
4. Loscalzo ML, Goh DL, Loeys B, Kent KC, Spevak PJ, Dietz HC. Familial thoracic aortic dilation and bicommissural aortic valve: a prospective analysis of natural history and inheritance. *Am J Med Genet A*. 2007;143A:1960-7.
5. Mahadevia R, Barker AJ, Schnell S, Entezari P, Kansal P, Fedak PW, et al. Bicuspid aortic cusp fusion morphology alters aortic three-dimensional outflow patterns, wall shear stress, and expression of aortopathy. *Circulation*. 2014;129:673-82.
6. Guzzardi DG, Barker AJ, van Ooij P, Malaisrie SC, Puthumana JJ, Belke DD, et al. Valve-related hemodynamics mediate human bicuspid aortopathy: insights from wall shear stress mapping. *J Am Coll Cardiol*. 2015;66:892-900.
7. Balint B, Yin H, Nong Z, Arpino JM, O'Neil C, Rogers SR, et al. Seno-destructive smooth muscle cells in the ascending aorta of patients with bicuspid aortic valve disease. *EBioMedicine*. 2019;43:54-66.
8. Noly PE, Basmadjian L, Bouhout I, Viet Le VH, Poirier N, El-Hamamsy I. New insights into unicuspid aortic valve disease in adults: not just a subtype of bicuspid aortic valves. *Can J Cardiol*. 2016;32:110-6.
9. Anderson RH. Understanding the structure of the unicuspid and unicommissural aortic valve. *J Heart Valve Dis*. 2003;12:670-3.
10. Mookadam F, Thota VR, Lopez AM, Emani UR, Tajik AJ. Unicuspid aortic valve in children: a systematic review spanning four decades. *J Heart Valve Dis*. 2010;19:678-83.
11. Roberts WC, Ko JM, Hamilton C. Comparison of valve structure, valve weight, and severity of the valve obstruction in 1849 patients having isolated aortic valve replacement for aortic valve stenosis (with or without associated aortic regurgitation) studied at 3 different medical centers in 2 different time periods. *Circulation*. 2005;112:3919-29.
12. Collins MJ, Butany J, Borger MA, Strauss BH, David TE. Implications of a congenitally abnormal valve: a study of 1025 consecutively excised aortic valves. *J Clin Pathol*. 2008;61:530-6.
13. Butany J, Vaideeswar P, Dixit V, Lad V, Vegas A, David TE. Ascending aortic aneurysms in unicommissural aortic valve disease. *Cardiovasc Pathol*. 2009;18:11-8.
14. Slostad BD, Witt CM, O'Leary PW, Maleszewski JJ, Scott CG, Dearani JA, et al. Unicuspid aortic valve: demographics, comorbidities, echocardiographic features, and long-term outcomes. *Circulation*. 2019;140:1853-5.
15. Henn D, Perttunen H, Gauer S, Schmied W, Porras C, Such M, et al. GATA5 and endothelial nitric oxide synthase expression in the ascending aorta is related to aortic size and valve morphology. *Ann Thorac Surg*. 2014;97:2019-25.
16. Won D, Zhu SN, Chen M, Teichert AM, Fish JE, Matouk CC, et al. Relative reduction of endothelial nitric-oxide synthase expression and transcription in atherosclerosis-prone regions of the mouse aorta and in an in vitro model of disturbed flow. *Am J Pathol*. 2007;171:1691-704.
17. Evangelista A, Flachskampf F, Lancellotti P, Badano L, Aguilar R, Monaghan M, et al. European Association of Echocardiography recommendations for standardization of performance, digital storage and reporting of echocardiographic studies. *Eur J Echocardiogr*. 2008;9:438-48.
18. Gauer S, Balint B, Kollmann C, Federspiel JM, Henn D, Bandner-Risch D, et al. Dysregulation of endothelial nitric oxide synthase does not depend on hemodynamic alterations in bicuspid aortic valve aortopathy. *J Am Heart Assoc*. 2020;9:e016471.
19. Henn D, Bandner-Risch D, Perttunen H, Schmied W, Porras C, Ceballos F, et al. Identification of reference genes for quantitative RT-PCR in ascending aortic aneurysms. *PLoS One*. 2013;8:e54132.
20. Giusti B, Sticchi E, De Cario R, Magi A, Nistri S, Pepe G. Genetic bases of bicuspid aortic valve: the contribution of traditional and high-throughput sequencing approaches on research and diagnosis. *Front Physiol*. 2017;8:612.
21. Kotlarczyk MP, Billaud M, Green BR, Hill JC, Shiva S, Kelley EE, et al. Regional disruptions in endothelial nitric oxide pathway associated with bicuspid aortic valve. *Ann Thorac Surg*. 2016;102:1274-81.
22. Mohamed SA, Radtke A, Saraei R, Bullerdiek J, Sorani H, Nimzyk R, et al. Locally different endothelial nitric oxide synthase protein levels in ascending aortic aneurysms of bicuspid and tricuspid aortic valve. *Cardiol Res Pract*. 2012;2012:165957.
23. Aicher D, Urbich C, Zeiher A, Dimmeler S, Schafers HJ. Endothelial nitric oxide synthase in bicuspid aortic valve disease. *Ann Thorac Surg*. 2007;83:1290-4.
24. Xiao Y, Liu Q, Han HC. Buckling reduces eNOS production and stimulates extracellular matrix remodeling in arteries in organ culture. *Ann Biomed Eng*. 2016;44:2840-50.
25. Steed MM, Tyagi N, Rodriguez W, Ovechkin A, Moshal K, Tyagi SC. Mechanisms of vascular remodeling in eNOS knockout mice. *FASEB J*. 2006;20:A711-2.
26. Barker AJ, Lanning C, Shandas R. Quantification of hemodynamic wall shear stress in patients with bicuspid aortic valve using phase-contrast MRI. *Ann Biomed Eng*. 2010;38:788-800.
27. Barker AJ, Markl M, Burk J, Lorenz R, Bock J, Bauer S, et al. Bicuspid aortic valve is associated with altered wall shear stress in the ascending aorta. *Circ Cardiovasc Imaging*. 2012;5:457-66.
28. Ma LE, Vali A, Blanken C, Barker AJ, Malaisrie C, McCarthy P, et al. Altered aortic 3-dimensional hemodynamics in patients with functionally unicuspid aortic valves. *Circ Cardiovasc Imaging*. 2018;11:e007915.
29. van Ooij P, Markl M, Collins JD, Carr JC, Rigsby C, Bonow RO, et al. Aortic valve stenosis alters expression of regional aortic wall shear stress: new insights from a 4-dimensional flow magnetic resonance imaging study of 571 subjects. *J Am Heart Assoc*. 2017;6:e005959.
30. Krepp JM, Roman MJ, Devereux RB, Bruce A, Prakash SK, Morris SA, et al. Bicuspid and unicuspid aortic valves: different phenotypes of the same disease? Insight from the GenTAC Registry. *Congenit Heart Dis*. 2017;12:740-5.
31. Lee TC, Zhao YD, Courtman DW, Stewart DJ. Abnormal aortic valve development in mice lacking endothelial nitric oxide synthase. *Circulation*. 2000;101:2345-8.
32. Wu J, Zafar MA, Li Y, Saeyeldin A, Huang Y, Zhao R, et al. Ascending aortic length and risk of aortic adverse events: the neglected dimension. *J Am Coll Cardiol*. 2019;74:1883-94.
33. Adriaans BP, Heuts S, Gerretsen S, Cheriex EC, Vos R, Natour E, et al. Aortic elongation part I: the normal aortic ageing process. *Heart*. 2018;104:1772-7.

Key Words: aortic valve disease, ascending aorta, aortopathy, unicuspid aortic valve, eNOS

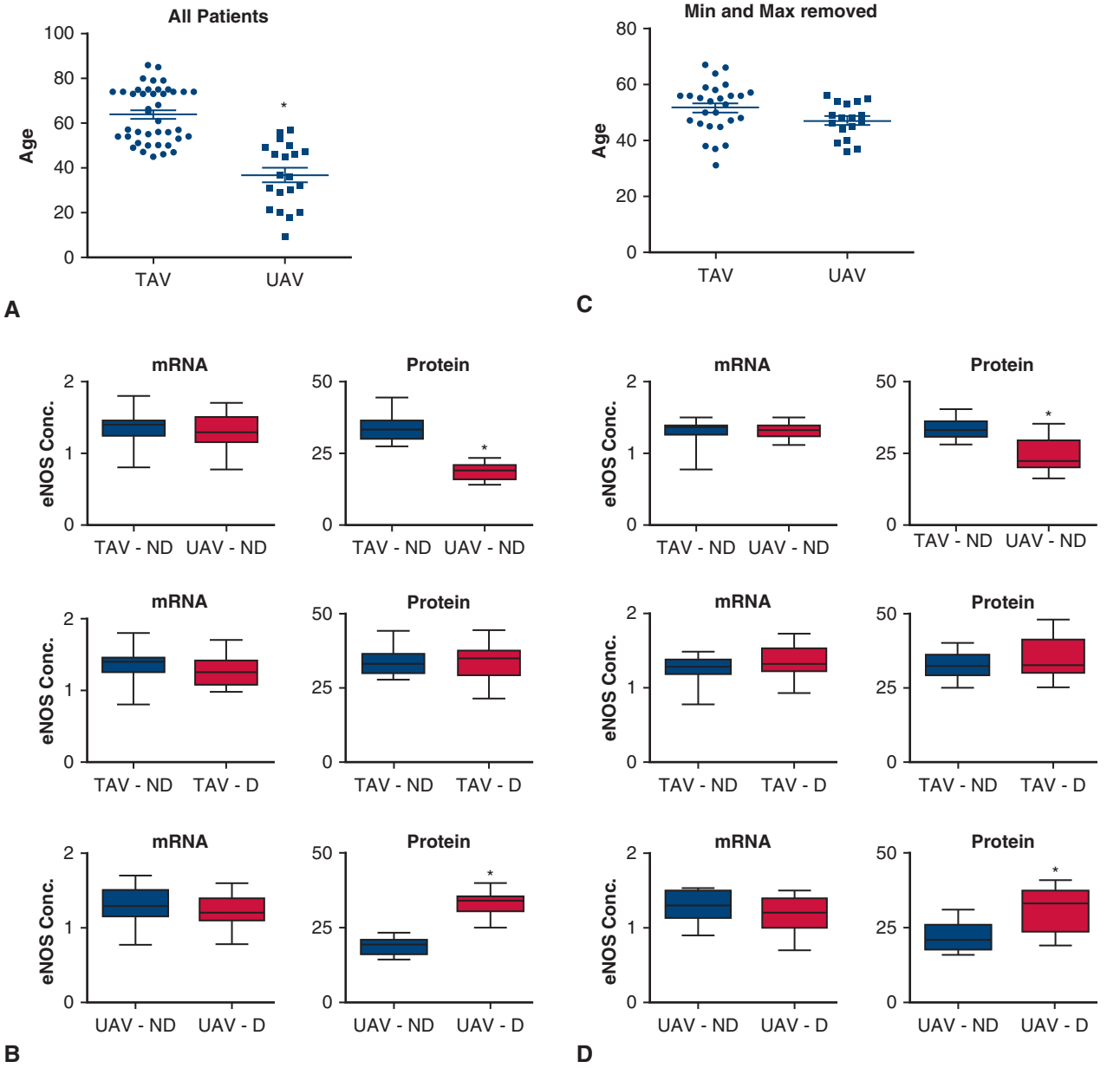

FIGURE E1. Comparison of original analysis and subanalysis after correcting for age. A, Graph depicting patient age for all patients with a tricuspid aortic valve (*TAV*) and with a unicuspid aortic valve (*UAV*). *$P < .0001$. B, *Box and whisker plots* comparing the mRNA (*left*) and protein (*right*) concentrations between groups with the original data set. *$P = .02$ and .04. *TAV-ND*: TAV–nondilated: N = 25, *TAV-D*: TAV–dilated: N = 17, *UAV-ND*: UAV–nondilated: N = 9, *UAV-D*: UAV–dilated: N = 13. C, Graph depicting patient age of TAV and UAV patients after removing the oldest 10 patients from the TAV group and the youngest 5 patients from the UAV group. $P = .08$. D, *Box and whisker plots* comparing the mRNA (*left*) and protein (*right*) concentrations between groups with the age-adjusted data set. *$P = .003$ and .011. TAV-ND: TAV–nondilated: N = 17, TAV-D: TAV–dilated: N = 14, UAV-ND: UAV–nondilated: N = 7, UAV-D: UAV–dilated: N = 10. In both the original data set and the age-adjusted data set, significant differences between groups were observed only in eNOS protein concentration between the TAV-ND and UAV-ND groups and the UAV-ND and UAV-D groups. *eNOS*, Endothelial nitric oxide synthase; *mRNA*, messenger RNA.